CSIRO PUBLISHING

Reproduction, Fertility and Development
http://dx.doi.org/10.1071/RD15200

Localisation of RNAs and proteins in nucleolar precursor bodies of early mouse embryos

Elena Lavrentyeva[A,B], *Kseniya Shishova*[A], *German Kagarlitsky*[A] *and Olga Zatsepina*[A,C]

[A]Shemyakin–Ovchinnikov Institute of Bioorganic Chemistry, Russian Academy of Sciences, Miklukho-Maklaya Street, 16/10, Moscow, 117997, Russian Federation.
[B]Faculty of Bioengineering and Bioinformatics, Lomonosov Moscow State University, GSP-1, Leninskiye Gory, MSU, 1-73, Moscow, 119991, Russian Federation.
[C]Corresponding author. Email: zatsepina_olga@mail.ru

Abstract. Early embryos of all mammalian species contain morphologically distinct but transcriptionally silent nucleoli called the nucleolar precursor bodies (NPBs), which, unlike normal nucleoli, have been poorly studied at the biochemical level. To bridge this gap, here we examined the occurrence of RNA and proteins in early mouse embryos with two fluorochromes – an RNA-binding dye pyronin Y (PY) and the protein-binding dye fluorescein-5′-isothiocyanate (FITC). The staining patterns of zygotic NPBs were then compared with those of nucleolus-like bodies (NLBs) in fully grown surrounded nucleolus (SN)-type oocytes, which are morphologically similar to NPBs. We show that both entities contain proteins, but unlike NLBs, NPBs are significantly impoverished for RNA. Detectable amounts of RNA appear on the NPB surface only after resumption of rDNA transcription and includes pre-rRNAs and 28S rRNA as evidenced by fluorescence *in situ* hybridisation with specific oligonucleotide probes. Immunocytochemical assays demonstrate that zygotic NPBs contain rRNA processing factors fibrillarin, nucleophosmin and nucleolin, while UBF (the RNA polymerase I transcription factor) and ribosomal proteins RPL26 and RPS10 are not detectable. Based on the results obtained and data in the contemporary literature, we suggest a scheme of NPB assembly and maturation to normal nucleoli that assumes utilisation of maternally derived nucleolar proteins but of nascent rRNAs.

Additional keywords: confocal laser-scanning microscopy, early mammalian development, FITC, fluorescence *in situ* hybridisation, immunofluorescence, NPBs, nucleolar proteins, nucleolus-like bodies (NLBs), pyronin Y, rRNA.

Received 19 May 2015, accepted 13 August 2015, published online 17 September 2015

Introduction

A mandatory feature of zygotic mammalian embryos that distinguishes them from embryos of other vertebrates is the presence of specific bodies called nucleolar precursor bodies (NPBs). NPBs appear in both pronuclei shortly after fertilisation as numerous (~10 in each pronucleus), small (~1 μm in diameter) optically dense roundish bodies randomly distributed in the nucleoplasm. During the zygotic stage, the number of NPBs decreases while their size increases, so that before the pronuclei fuse, a single large (~10 μm in diameter) NPB is usually seen in each pronucleus (Fulka and Fulka 2010; Kyogoku *et al.* 2014*a*; 2014*b*). The time of NPB assembly and the pattern of their localisation are used as biomarkers of developmental potencies of human embryos (Fulka and Fulka 2010; Papale *et al.* 2012). Mechanisms underlying the assembly and fusion of NPBs are presently unknown, but mitogen-activated protein kinase (MAPK) and maturation promoting factor (MPF) activities may be involved (Li *et al.* 2012).

At the ultrastructural level, zygotic NPBs differ essentially from normal somatic nucleoli, but they look very similar to nucleolus-like bodies (NLBs) of surrounded nucleolus (SN)-type fully grown (germinal vesicle, GV) oocytes. NPBs, like NLBs, are comprised of a tightly packed fibrous material, lack the typical nucleolar tripartite organisation and are transcriptionally silent despite their association with ribosomal genes (rDNA; Fakan and Odartchenko 1980; Tesarík *et al.* 1987; Fléchon and Kopecný 1998; Laurincik *et al.* 2000; Romanova *et al.* 2006*b*; Bonnet-Garnier *et al.* 2012). The morphology of NPBs remains unchanged until the main resumption of rDNA transcription commences in late two-cell stage in the mouse (Engel *et al.* 1977; Zatsepina *et al.* 2003; Bogolyubova 2011) and in more advanced developmental stages in embryos of other mammalian species (Braude *et al.* 1988; Hyttel *et al.* 2000; Bjerregaard *et al.* 2004; Graf *et al.* 2014).

Resumption of rRNA synthesis initiates maturation (transformation) of transcriptionally silent NPBs into functional

nucleoli. Topologically, the transformation commences on the NPB surface, which starts to incorporate precursors of RNA synthesis (Hyttel *et al.* 2000; Zatsepina *et al.* 2003). Simultaneously, on the NPB surface the typical nucleolar subdomains (i.e. fibrillar centres, the dense fibrillar component and the granular component) become visible by electron microscopy and nucleolar proteins can be detected by immunocytochemical approaches (Geuskens and Alexandre 1984; Fléchon and Kopecný 1998; Laurincik *et al.* 2003; Zatsepina *et al.* 2003; Romanova *et al.* 2006*a*; Fulka and Langerova 2014). The peripheral tripartite nucleolus-like zone becomes more prominent, while the central fibrous part of maturing NPBs diminishes at every post-cleavage cycle so that by late morula or early blastocyst stages NPBs completely evolve to normal tripartite nucleoli (Geuskens and Alexandre 1984; Laurincik *et al.* 2000, 2003). Formation of normal nucleoli coincides with the bulk expression of embryonic genes (Wang *et al.* 2004; Zeng and Schultz 2005; Hamatani *et al.* 2006; Rodriguez-Zas *et al.* 2008; Duncan and Schultz 2010; Graf *et al.* 2014). However, whether the assembly of nuclei occurs in all blastomeres simultaneously or whether it is coordinated with the onset of blastomer differentiation that commences prior the morula–blastocyst stages (Oestrup *et al.* 2009; Morris and Zernicka-Goetz 2012) remains unexamined.

The ultrastructural resemblance and transcriptional silencing for a long time supported the idea that zygotic NPBs and oocyte NLBs are comprised of the same molecular constituent and therefore are closely related or even analogous structures. Numerous studies were undertaken to prove this idea by determining NPB and NLB molecular composition (Biggiogera *et al.* 1994; Baran *et al.* 1995; Ferreira and Carmo-Fonseca 1995; Laurincik *et al.* 2003; Zatsepina *et al.* 2000, 2003; Bjerregaard *et al.* 2004; Romanova *et al.* 2006*a*; Svarcova *et al.* 2009; Vogt *et al.* 2012). However, these efforts mostly failed, as far as under standard immunolabelling conditions the inner mass of NPBs and NLBs remained almost unstained. Recently, by modification of standard immunostaining assays it has been shown that zygotic NPBs, like oocyte NLBs, contain nucleolar proteins NPM1 (B23, nucleophosmin), C23 (nucleolin) and fibrillarin but apparently lack the RNA polymerase I cofactor UBF (Fulka and Langerova 2014; Shishova *et al.* 2015). These observations support the above-mentioned idea but they do not explain why microsurgical removal of zygotic NPBs does not affect further embryonic development (Kyogoku *et al.* 2014*a*; 2014*b*), whereas enucleolated GV oocytes are incapable of giving rise to fully developed embryos (Ogushi *et al.* 2008; Ogushi and Saitou 2010).

In contrast to proteins, the presence of RNA inside NPBs is very poorly studied. Early autoradiographic observations showed that a certain amount of long-lived maternal RNA is present in zygotic NPBs of mouse and hamster embryos (Biggiogera *et al.* 1994; Kopečný *et al.* 1995). However, types of the oocyte-derived RNAs were unascertained and these early observations have not been reinvestigated by other approaches.

An objective of the current work has been to examine the occurrence of RNA and proteins in zygotic NPBs and throughout their transformation to mature nucleoli in mouse embryos. To this end, we stained the embryos with a fluorescent RNA-binding dye pyronin Y (PY; Darzynkiewicz *et al.* 1987; Kapuscinski and Darzynkiewicz 1987) and with the protein-binding dye, fluorescein-5′-isothiocyanate (FITC; Shishova *et al.* 2015). Our results show that NPBs, unlike NLBs, are very weakly stained with PY, i.e. are impoverished for RNA, while both entities are intensely stained with FITC and thus contain proteins. Clearly detectable RNA appears at the NPB surface only after resumption of rRNA synthesis as is demonstrated by PY staining and by fluorescence *in situ* hybridisation (FISH) with specific oligonucleotide probes targeting rRNA. We also show that NPBs contain rRNA processing factors NPM1, nucleolin and fibrillarin, but do not contain UBF and ribosomal proteins RLP26 and RPS10. Thus, our results show that the biochemical composition of zygotic NPBs and oocyte NLBs differs and, therefore, that NPBs and NLBs are not fully analogous structures. We assume that maturing NPBs incorporate the maternally inherited nucleolar proteins but the newly synthesised rRNA. A scheme illustrating the assembly and maturation of NPBs to typical nucleoli in mouse embryos is proposed.

Materials and methods

Animals

Female and male C57Bl/6 mice were purchased from the Pushchino Nursery of Laboratory Animals (Pushchino, Russia). The animals were kept under pathogen-free conditions with access to standard chow and tap water *ad libitum*. All experiments were performed according to the local regulations based on the Directive 2010/63/EU on the protection of animals used for scientific purposes.

Collection of embryos and oocytes

Four-to-six-week-old females were used. To obtained embryos, the females were injected with 7 IU pregnant mare serum gonadotrophin (PMSG; Sigma-Aldrich, St Louis, MO, USA) followed by 7 IU human chorionic gonadotrophin (hCG; Sigma-Aldrich) 46–48 h later and caged with males. Females were sacrificed and embryos were collected in M2 medium (Sigma-Aldrich) at different time intervals after hCG injection according to Bouniol *et al.* (1995). Early and late zygotes were collected 20–21 h and 27–29 h after hCG injection, respectively, from ampullae. Late two-cell embryos were collected at 48–49 h after hCG and four-cell embryos were collected at 59–60 h after hCG from oviducts. Eight-cell and multi-cell morula embryos were collected 67–68 h and 80–84 h after hCG, respectively. Embryos at the blastocyst stage were obtained by *in vitro* culture of multicell embryos in EmbryoMax KSOM Medium (Merck Millipore, San Diego, CA, USA) at 37°C and 5% CO_2. Fully grown oocytes were obtained from PMSG-injected females by gentle puncturing of ovaries in M2 medium supplemented with 100 μg mL^{-1} dibutyryl-cAMP (dbcAMP; Santa Cruz Biotechnology Inc., Santa Cruz, CA, USA) to prevent resumption of meiosis. Oocytes were denuded by pipetting in M2 supplemented with dbcAMP and 0.1% hyaluronidase.

Pyronin Y and FITC staining

Zygotes and GV oocytes were fixed with 3% paraformaldehyde (PFA) in phosphate-buffered saline (PBS) for 30 min at room

Table 1. Oligonucleotide probes used in FISH analysis and the probe positions along the mouse 47S pre-rRNA

Probe	Sequence 5′ to 3′	Position
5′ETS	Antisense: Cy3-ATCGGGAGAAACAAGCGAGATAGGAATGTCTTA Sense: Cy3-TAAGACATTCCTATCTCGCTTGTTTCTCCCGAT	602–634
ITS1	Antisense: Cy3-AAACCTCCGCGCCGGAACGCGACAGCTAGG Sense: Cy3-GGCCGGTGGGTCGCCTGCGGTTGTCTG	6391–6420
28S	Antisense: FAM-GAGGGAACCAGCTACTAGATGGTTCGATTA Sense: FAM-TAATCGAACCATCTAGTAGCTGGTTCCCTC	9571–9600

temperature, washed in PBS (3 × 10 min) and permeabilised with 0.2% Triton X-100 in PBS for 20 min on ice. They were then stained in a mixture of 10 μg mL^{-1} PY (Sigma-Aldrich) and 1 μg mL^{-1} FITC (fluorescein-5′-isothiocyanate isomer I; Biotium Inc., Hayward, CA, USA) in PBS for 2 h at room temperature, counterstained with 1 μg mL^{-1} 4’,6-diamidino-2-phenylindole, dihydrochloride (DAPI) for 10–15 min and mounted in Vectashield (Vector Laboratories Inc., Burlingame, CA, USA).

To examine the specificity of PY staining, PFA-fixed and Triton X-100-permeabilised cells were treated with 1 mg mL^{-1} RNase A (Sigma-Aldrich) in PBS for 2 h before exposure to the dye. The specificity of FITC staining was monitored by pre-incubation of oocytes (embryos) with 1 μg mL^{-1} proteinase K (Sigma-Aldrich) in PBS for 30 min at room temperature (20–23°C). In control groups, oocytes and embryos were incubated in PBS during the same time and at the same temperature as the treated cells.

Fluorescence in situ *hybridisation*

Fluorescence *in situ* hybridisation (FISH) was performed with antisense oligonucleotide probes targeting the mouse 47S pre-rRNA (Table 1). The 5′ETS probe targets the short-lived segment of the 5′-external transcribed spacer (5′ETS; Lazdins *et al.* 1997; Mullineux and Lafontaine 2012), the ITS1 probe recognises unprocessed rRNA and the 28S rRNA probe hybridises with the 28S rRNA region. The sense probes were used as the negative controls (Table 1). The 5′ETS and ITS1 antisense and sense probes were conjugated with Cy3 and the 28S rRNA probes were conjugated with fluorescein (FAM) at the 5′-terminal end. The probes were synthesised by DNA-synthesis Ltd (Moscow, Russia). The concentration of the probes in stock solutions was 2 μg μL^{-1}. To minimise putative artefacts that can be caused by fixation, two different approaches were applied. (1) Embryos were fixed with 70% ethanol for 20 min at room temperature, washed with PBS (3 × 5–7 min) and treated with 0.2% Triton X-100 (10 min at 4°C). (2) Embryos were fixed with PFA as described above for the PY and FITC staining. In both cases, after brief washing in PBS embryos were washed in 2× saline–sodium citrate buffer (SSC; 0.3M NaCl, 0.03 M $Na_3C_6H_5O_7$, pH 7.0; 2 × 10 min) and transferred to the hybridisation mixture containing 50% deionised formamide (Sigma-Aldrich), 10% dextran sulfate (Loba Chemie, Fischamend, Austria), 5% 20× SSC (3 M NaCl, 0.3 M $Na_3C_6H_5o_7$, pH 7.0) and 8 ng mL^{-1} oligonucleotide probes. Hybridisation was performed in a wet chamber for 18 h at 42°C. Before mounting in Vectashield, embryos were sequentially washed with 50% formamide (Panreac, Barcelona, Spain) dissolved in 2× SSC at 42°C (3 × 10 min), 2× SSC at 42°C (10 min) and in 2× SSC at room temperature (10 min). In some experiments, after hybridisation embryos were immunolabelled with antibodies against a nucleolar protein nucleolin.

Over 15 zygotes were hybridised with every FISH probe (Table 1).

Immunolabelling

Zygotes were fixed with 3% PFA, permeabilised with 0.2% Triton X-100 for 10 min and transferred to 1 μg mL^{-1} proteinase K (Sigma-Aldrich) in PBS for 20–30 min at room temperature (Shishova *et al.* 2015). After washing in PBS (3 × 10 min), embryos were incubated with antibodies against UBF (Zatsepina *et al.* 1993), fibrillarin (ab5821; Abcam, Cambridge, UK), NPM1 (B0556; Sigma-Aldrich), nucleolin (ab70493; Abcam), RPL26 (ab59567; Abcam) or RPS10 (ab151550; Abcam). The following secondary antibodies were used: goat anti-human IgG conjugated with FITC (F3512; Sigma-Aldrich; to detect UBF), Alexa Fluors 488 goat anti-rabbit IgG (A-11034; Molecular Probes Inc., Eugene, OR, USA; to detect fibrillarin, nucleolin, RPL26, RPS10) and Alexa Fluors 488 goat anti-mouse IgG (A11029; Molecular Probes Inc.; to detect NPM1). All antibodies were dissolved in PBS following recommendations of the suppliers and the immunolabelling steps were performed at room temperature for 45 min–1 h. The embryos were washed in PBS (3 × 10 min), stained with 1 μg mL^{-1} DAPI for 10–15 min and mounted in Vectashield. Over 15 zygotes were immunolabelled with each primary antibody.

Confocal imaging and fluorescent signal quantification

In all cases, eight-bit images of single optical sections were acquired with a DuoScanMeta LSM510 confocal laser scanning microscope (Carl Zeiss, Göttingen, Germany) and a Plan-Apochromat 63× /1.40 numerical aperture immersion lens (Carl Zeiss).

Images of PY- and FITC-stained cells were acquired with the following parameters: for PY fluorescence (RNA staining), excitation at 514 nm and emission at 530 nm; for FITC fluorescence (protein staining), excitation at 488 nm, emission at 505–550 nm. To quantify fluorescent signals, images of single optical sections of the PY- or FITC-stained oocytes (embryos) were recorded with the same laser power output and the image acquisition parameters that were adjusted for each of the dyes

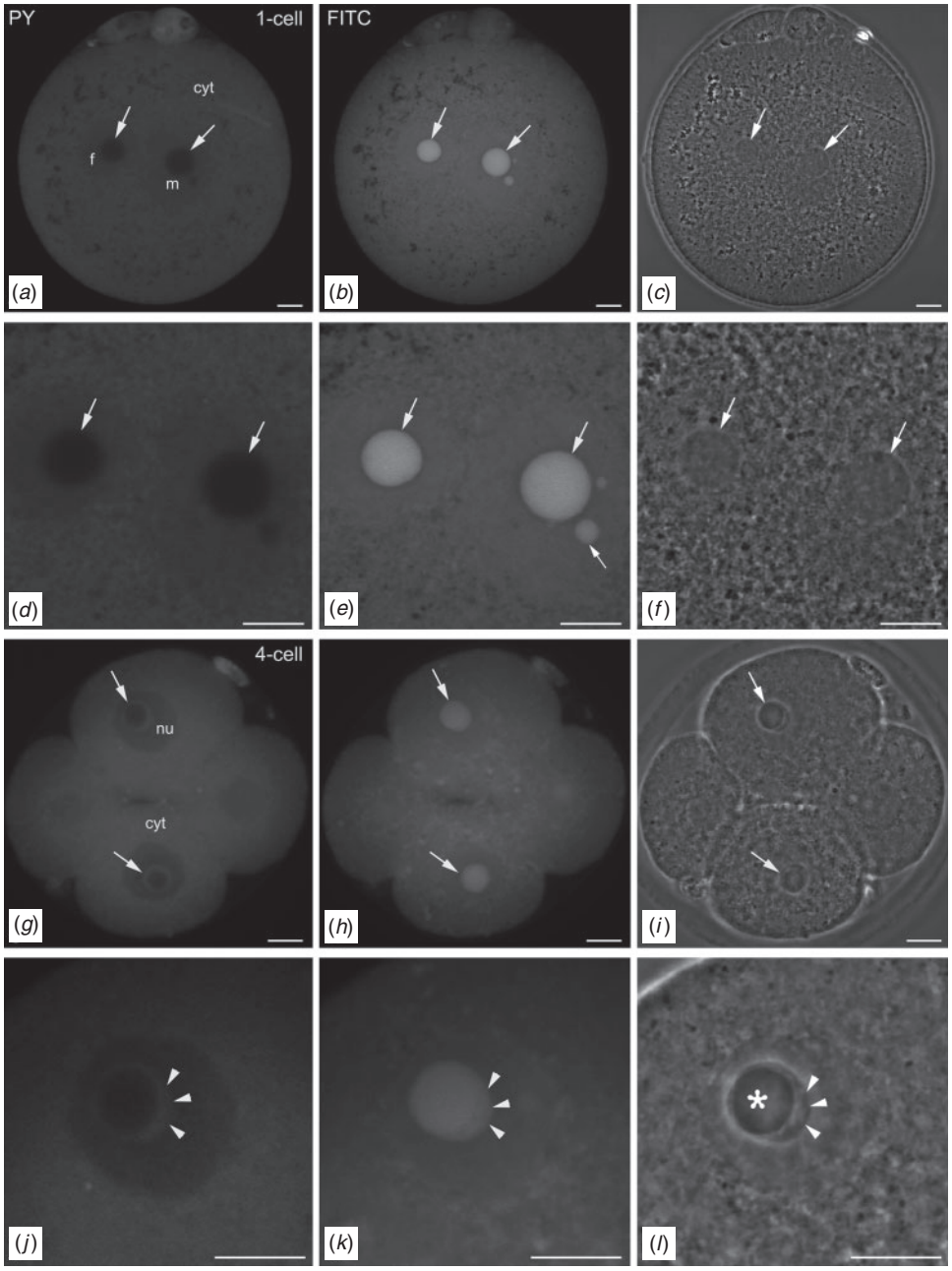

Fig. 1. Mouse embryos simultaneously stained with (*a*, *d*, *g*, *j*) a fluorescent RNA-binding dye pyronin Y and (*b*, *e*, *h*, *k*) the fluorescent protein-binding dye FITC in (*a–f*) late zygote (28 h after hCG) and (*g–l*) at the 4-cell stage. (*c*, *f*, *i*, *l*) Phase-contrast images. f, female pronucleus; m, male pronucleus; cyt, cytoplasm; nu, nucleus; arrows indicate nucleolar precursor bodies (NPBs); arrowheads indicate an optically light rim at the NPB surface; * indicates the optically dense NPB core. Zygotic NPBs and the core of maturing NPBs are very weakly stained with PY being intensely stained with FITC. The PY-positive rim at the NPB periphery is weaker stained with FITC than the NPB core (in (*j–l*) the upper of the two NPBs seen in (*g–i*) is shown). Scale bars = 10 μm.

using the control (untreated) cells. The cells examined included: after PY staining, control oocytes ($n = 10$), RNase A-treated oocytes ($n = 8$), control zygotes ($n = 10$), RNase A-treated zygotes ($n = 8$); after FITC staining, control oocytes ($n = 8$), proteinase K-treated oocytes ($n = 8$), control zygotes ($n = 10$), proteinase K-treated zygotes ($n = 11$). In every group, 3–5 images of oocytes and zygotes were recorded. Image J software (http://imagej.nih.gov/ij/download.html) was used to ascertain the fluorescence intensity per pixel in the regions-of-interest (ROIs) such as NLBs and NPBs. Background fluorescence was

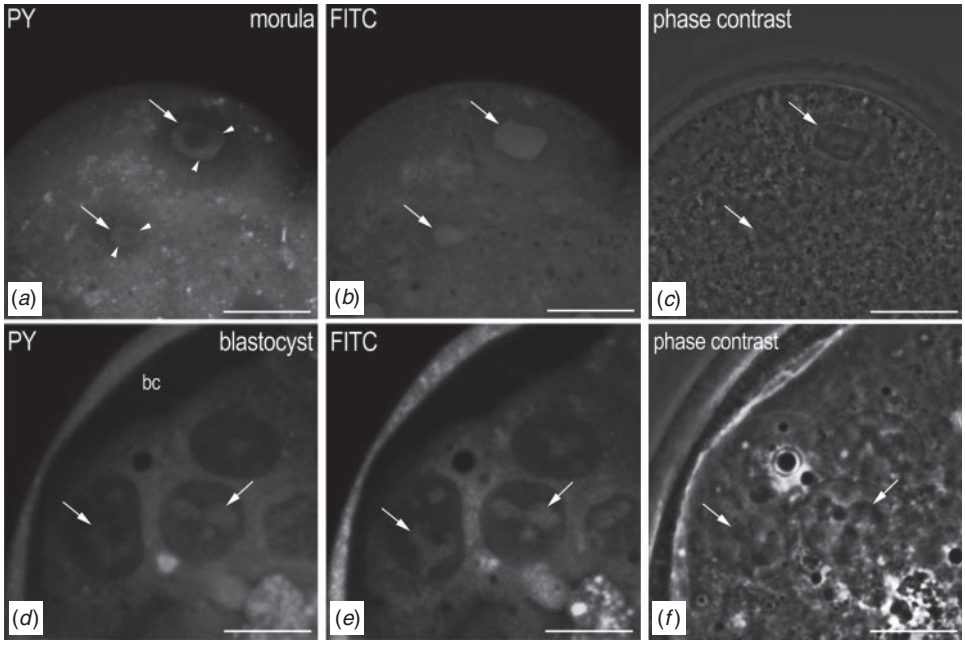

Fig. 2. Mouse embryos stained with (*a*, *d*) PY and (*b*, *e*) FITC at the (*a–c*) morula and (*d–f*) blastocyst stages. (*c*,*f*) Phase-contrast images. bc, blastocyst cavity; (*a–c*) arrows indicate maturing NPBs; (*d–f*) arrows indicate mature nucleoli; (*a*) arrowheads indicate the PY-stained peripheral NPB zone. The PY-negative core of maturing NPBs is reduced as compared with that in four-cell embryos and completely disappears in blastocyst nucleoli. Scale bars = 10 μm.

measured in arbitrary-sized ROIs outside oocytes or embryos. The values obtained were displayed in 0–255 greyscale (Shishova *et al.* 2015). Over 30 measurements per treatment condition and in the untreated controls were made. The average pixel fluorescence intensities and corresponding standard deviations (s.d.) were calculated and the values obtained were compared by *t*-test using Microsoft Office Excel 2007 software (Microsoft Corp., Redmond, WA, USA).

Results

PY and FITC staining of mouse embryos and oocytes

Fig. 1 shows representative one-cell ($n = 12$) and four-cell ($n = 11$) embryos that were simultaneously stained with PY (Fig. 1*a*, *d*, *g*, *j*) and FITC (Fig. 1*b*, *e*, *h*, *k*). In the embryos, both dyes stain the cytoplasm and the nucleoplasm, but the pattern of NPB staining depends on the dye and the embryonic stage. In zygotes, NPBs are almost unstained with PY (Fig. 1*a*, *d*) but are brightly and homogeneously stained with FITC (Fig. 1*b*, *e*). Under phase contrast, the NPB mass looks rather uniform (Fig. 1*c*, *f*). In four-cell embryos (Fig. 1*g–l*), when rDNA transcription is known to resume (Engel *et al.* 1977; Zatsepina *et al.* 2003), two NPB zones – the core part and the peripheral rim – become visible after staining with both dyes. Therein, the NPB periphery is conspicuously stained with PY, whereas the central zone is unstained similar to zygotic NPBs (Fig. 1*g*, *j*). Unlike PY, FITC more brightly stains the NPB core than the NPB periphery (Fig. 1*h*, *k*). The PY-bright and FITC-weak peripheral rim coincides with a more transparent zone observed under phase contrast (Fig. 1*i*, *l*). The peripheral zone most likely corresponds to the nucleolus-like part of activated NPBs, whereas the NPB central part contains a fibrous material comprising zygotic NPBs. The PY-negative core remains visible in NPBs in morula embryos ($n = 11$; Fig. 2*a–c*) but disappears at the blastocyst stage ($n = 10$; Fig. 2*d–f*).

To compare the patterns of PY and FITC staining in zygotic NPBs with those in NLBs, SN-type oocytes ($n = 12$) were incubated in a mixture of PY and FITC under the conditions used for staining zygotes. In Fig. 3, a typical SN-type oocyte is shown. Similar to NPBs (Fig. 1*b*, *e*), NLBs are brilliantly stained with FITC (Fig. 3*b*), but in contrast to NPBs (Fig. 1*a*, *d*) they are also stained with PY (Fig. 3*a*). The quantification of PY signals in NPBs and NLBs (Fig. 4*a*) shows that the PY average fluorescence intensity per pixel in NPBs is almost one-third that in NLBs ($P < 0.001$; Fig. 4*a*). In somatic cells, PY specifically binds RNA (Kapuscinski and Darzynkiewicz 1987) but its specificity in mouse oocytes and embryos has not been studied thus far. To examine whether PY also stains RNA in these conditions, we incubated PFA-fixed oocytes (embryos) in a 1 mg mL^{-1} solution of RNase A in PBS or in PBS alone (the control), stained the cells and quantified PY fluorescence as described in Materials and Methods. Fig. 4*a* shows that PY staining in NLBs is noticeably sensitive to the enzyme (Fig. 4*a*) thus evidencing that PY binds RNA under our conditions. A residual PY fluorescence retained in NLBs and NPBs after RNase A treatment indicates that a part of their RNA may be tightly bound with proteins that protect RNA from digestion. The FITC fluorescence intensities in NPBs and NLBs in the

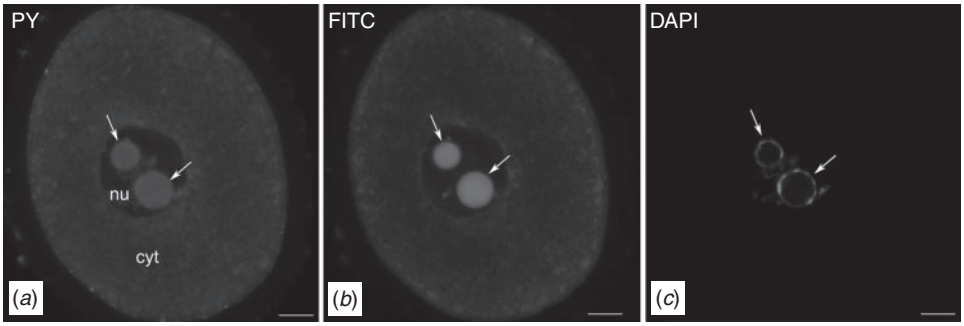

Fig. 3. A mouse GV SN-type oocyte with two nucleolus-like bodies (NLBs) that was stained with (*a*) PY and (*b*) FITC and then (*c*) counterstained with DAPI to determine the oocyte type. cyt, cytoplasm; nu, nucleus; arrows indicate NLBs. NLBs are stained with PY and FITC. Scale bars = 10 μm.

control and after treatment with proteinase K are illustrated in Fig. 4*b*. It shows that proteinase K significantly abolishes FITC fluorescence in both NPBs and NLBs (in both cases, $P < 0.001$) thereby proving that each of them contains proteins.

To find out whether RNA detected in NPBs with PY includes rRNA, we performed FISH with probes targeting the short-lived 5′ETS fragment of the 47S precursor rRNA (a marker of pre-rRNA synthesis), ITS1 (a marker of unprocessed rRNAs) and 28S rRNA, which hybridises with both unprocessed and processed rRNAs (Table 1). No FISH signals were seen in NPBs in zygotic embryos fixed with PFA (data not shown) and only weak 28S rRNA-FISH signals were observed in ethanol-fixed zygotes. Fig. 5 shows a representative ethanol-fixed zygote ($n = 15$) immunostained for nucleolin (Fig. 5*a*) and hybridised with the probe to 28S rRNA (Fig. 5*b*). In each pronucleus, several nucleolin-positive NPBs are visible (Fig. 5*a*), but most of them are weakly labelled (if at all) for 28S rRNA (Fig. 5*a*, *b*, asterisks). In none of the one-cell embryos ($n = 24$) did NPBs hybridise with the 5′ETS (Fig. 6*a*) or the ITS1 (Fig. 6*c*, *e*) probes. In contrast, in late two-cell (Fig. 5*c–e*) and in four-cell (Fig. 5*f–h*) embryos, which are known to transcribe rDNA (Engel *et al.* 1977; Zatsepina *et al.* 2003), 5′ETS (Fig. 5*c*, *e*), ITS1 (Fig. 5*f*, *h*) and 28S rRNA (Fig. 5*d*, *e*, *g*, *h*) signals become clearly visible on the NPB periphery. In NPBs of multi-cell embryos (Fig. 5*i*, *j*), 28S rRNA signals are visually more intense than the signals observed in zygotic NPBs (Fig. 5*b*).

To examine whether in zygotic embryos rRNA processing factors follow the same occurrence as rRNAs, we used embryos fixed with 70% ethanol ($n = 21$) and the embryos that were fixed with PFA and then treated with proteinase K ($n = 53$). The most convincing results were obtained in PFA-fixed and proteinase K-treated embryos, where in contrast to ethanol-fixed zygotes, chromatin was rather well preserved and was brightly stained with DAPI. The latter helped to identify distinct NPBs (Fig. 7), which shows that in one-cell embryos NPBs are clearly immunolabelled for fibrillarin (Fig. 7*a*, *j*), NPM1 (Fig. 7*c*, *k*) and nucleolin (Fig. 7*e*). Surprisingly, in early zygotes, some NPBs did not contain fibrillarin (Fig. 7*a*, *b*), albeit all zygotic NPBs were intensely labelled for NPM1 and nucleolin (Fig. 7*c*, *d*, *e*, *f*). In late zygotes, when only one or two large NPBs were present in each pronucleus, NPBs always contained fibrillarin (Fig. 7*j*, *l*). However, NPBs of neither early nor late zygotes were labelled

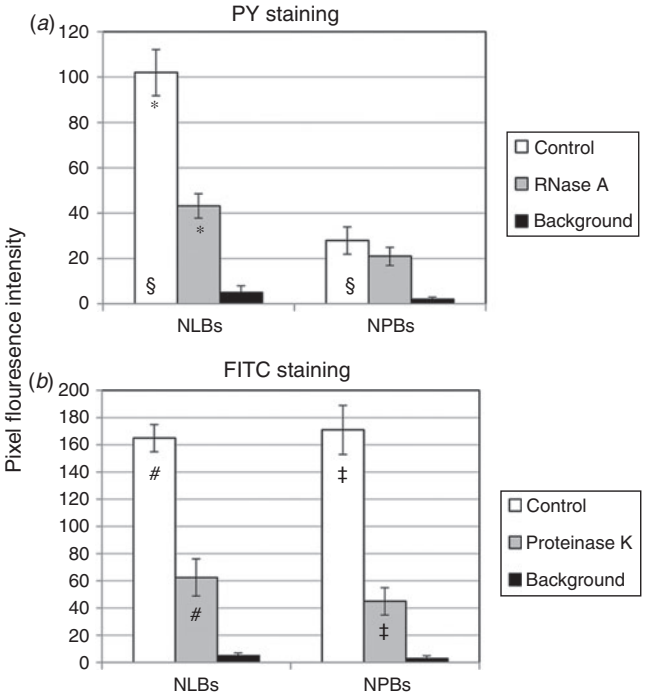

Fig. 4. Bar graphs illustrating (*a*) PY and (*b*) FITC fluorescence intensities per pixel in NLBs of GV oocytes and NPBs of zygotic embryos in the control (untreated cells) and after (*a*) RNase A or (*b*) proteinase K treatment. Oocytes and embryos of the control groups were incubated in PBS and oocytes (embryos) of the experimental groups were incubated in PBS containing 1 μg mL^{-1} RNase A for 2 h or 1 μg mL^{-1} proteinase K for 30 min at room temperature (20–23°C). Oocytes (embryos) were then stained with each dye and eight-bit digital images of the cells were acquired with the same laser output and image acquisition parameters. The pixel fluorescence intensities were measured in ROIs (regions-of-interest) and displayed as 0–255 greyscale values (see Materials and Methods for detail). In each compared group, ≥30 measurements were performed. Symbols (*, #, §, ‡) indicate the compared values that differ statistically (*t* test, $P < 0.001$). The PY fluorescence intensity in NPBs is ~3-fold lower than that in NLBs. The FITC fluorescence intensities in NPBs and NLBs do not differ significantly and are reduced by proteinase K. The specificity of RNA staining with PY is evidenced by essential reduction of PY fluorescence in NLBs treated with RNase A as compared with that in the untreated controls.

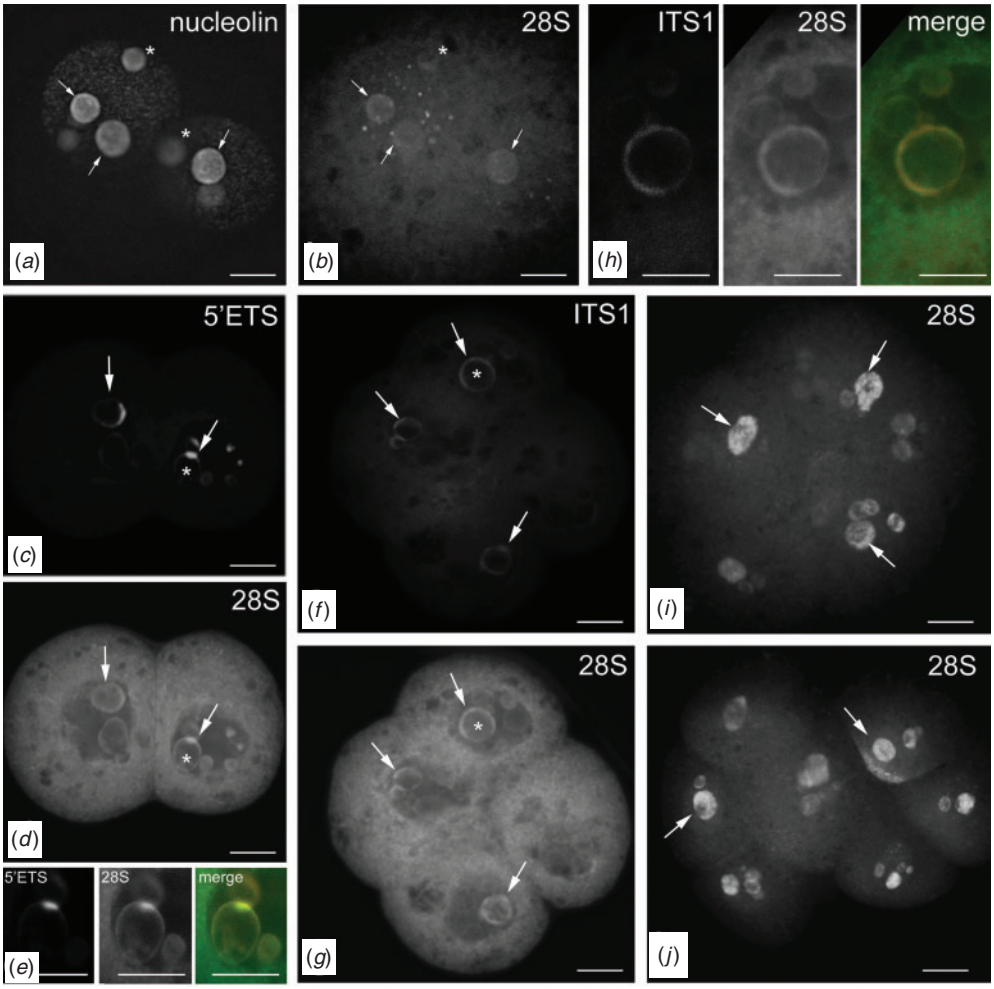

Fig. 5. Fluorescence *in situ* hybridisation of mouse embryos in (*a*, *b*) early one-cell, (*c–e*) late two-cell, (*f–h*) four-cell and (*i*, *j*) eight-cell (early morula) stages with the probes targeting (*b*, *d*, *e* (middle, right), *g*, *h* (middle, right), *i*, *j*) 28S rRNA, (*c*, *e* (left, right)) the short-lived 5′ETS end of the 47S precursor rRNA or (*f*, *h* (left, right)) ITS1. The embryo shown in (*a*, *b*) is also immunolabelled for nucleolin (*a*). The embryos shown in (*a*, *b*, *i*, *j*) were fixed with 70% ethanol and those shown in (*c–h*) were fixed with 3% paraformaldehyde. Small arrows indicate transcriptionally silent NPBs, long arrows indicate transcriptionally active NPBs. (*a*, *b*) Asterisks indicate NPBs with low (if any) detectable 28S rRNA signals; (*c*, *d* and *f*, *g*) asterisks indicate NPBs shown at a higher magnification in (*e*) and (*h*), respectively. In NPBs, FISH signals targeting the nascent 47S pre-rRNA (recognised with the 5′ETS probe), unprocessed rRNAs (the ITS1 and 28S rRNA probes) and 28S rRNA (the 28S rRNA probe) are clearly detectable from the late two-cell stage (*c–j*) onward. In two-cell and four-cell embryos, the signals are clearly detected only on the NPB surface (*e, h*). Scale bars = 10 μm.

with antibodies to the RNA polymerase transcription factor UBF (Fig. 7*g*) and ribosomal proteins RPL26 (Fig. 7*h*) or RPS10 (data not shown). It is worth mentioning that proteinase K treatment, in addition to visualisation of fibrillarin in NPBs, led to the appearance of numerous tiny fibrillarin-positive dots in the nucleoplasm of zygotic pronuclei. We did not observe similar signals with the other antibodies used in the study (Fig. 7*c*, *e*, *g*, *h*) and, despite numerous efforts, were unable to abolish their appearance. We assume that the nucleoplasmic fibrillarin foci could result from displacement of weakly bound fibrillarin molecules or fibrillarin fragments, which retained antigenic determinants, from NPBs to the nucleoplasm. Alternatively, they may be caused by recovery of hidden nuclear fibrillarin-containing sites. In the latter case, the nucleoplasmic fibrillarin may be functional: fibrillarin is the main nucleolar methyltransferase that in mouse embryos was described in Cajal bodies assembled before re-initiation of rRNA synthesis (Ferreira and Carmo-Fonseca 1995; Zatsepina *et al.* 2003). In one-cell embryos, fibrillarin-containing Cajal bodies co-localise with mRNA splicing factors and therefore were suggested to participate in mRNA processing (Ferreira and Carmo-Fonseca 1995). We cannot exclude, therefore, that the nucleoplasmic fibrillarin-positive dots, which we regularly observed in zygotic nuclei, could play a similar role.

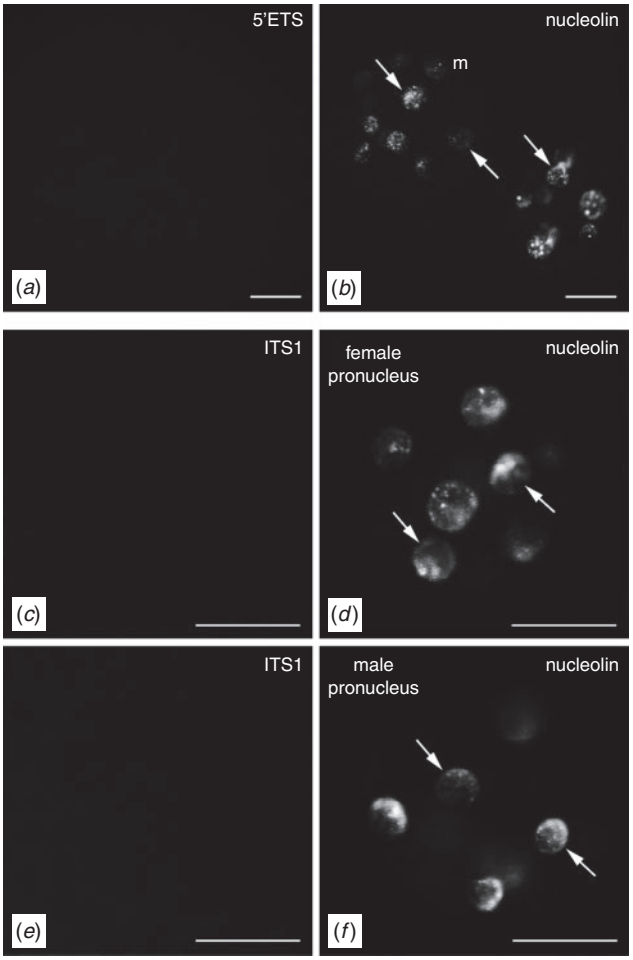

Fig. 6. Fluorescence *in situ* hybridisation of early zygotes with the probes targeting the (*a*) 5′ETS or (*c*, *e*) ITS1 fragments of the mouse 47S pre-rRNA combined with immunolabelling with antibodies against (*b*, *d*, *f*) nucleolin. In (*c*–*f*), two pronuclei of the same embryo are shown. f, female pronucleus; m, male pronucleus. In parental pronuclei, numerous nucleolin-positive but rRNA-negative NPBs are seen (arrows). Scale bars = 10 μm.

Discussion

The results of this study allow us to make the following main conclusions: (1) zygotic NPBs, unlike NLBs of GV oocytes, are significantly impoverished for RNA, as is evidenced by their weak staining with an RNA-binding dye pyronin Y (Fig. 1*a*, *d* and Fig. 3*a*, Fig. 4*a*), (2) zygotic NPBs, like NLBs, contain a vast amount of protein, as judged by a brilliant staining of both entities with the protein-binding dye FITC (Fig. 1*b*, *e*, Fig. 3*b*, Fig. 4*b*), (3) zygotic NPBs contain rRNA processing factors fibrillarin, NPM1 and nucleolin but lack the RNA polymerase I transcription factor UBF and ribosomal proteins RPL26 and RPS10 (Fig. 7), (4) resumption of rRNA synthesis in late two-cell embryos leads to the appearance of rRNAs on the NPB surface (Fig. 5*c*–*h*), (5) rRNAs occupy the whole NPB volume in the process of NPB transformation to normal nucleoli in multi-cell embryos (Fig. 5*i*, *j*) and (6) 28S rRNA-FISH signals are more evident in NPBs of four-cell (Fig. 5*i*) and multi-cell (Fig. 5*j*) embryos than in one-cell embryos (Fig. 5*b*), thus favouring the assumption that re-initiation of rRNA synthesis results in accumulation of rRNA in maturing NPBs.

For a long time, NPBs of zygotic embryos and NLBs of GV oocytes were considered as closely related or even alike structures. However, recent analysis of developmental capacities of mouse embryos obtained from enucleolated GV oocytes (Ogushi *et al.* 2008; Ogushi and Saitou 2010) and NPB-less zygotes (Kyogoku *et al.* 2014*a*, 2014*b*) indicated that functional and biochemical similarities between NPBs and NLBs are most likely overestimated. Indeed, embryos obtained from the enucleolated oocytes stopped development at the two- or four-cell stages, whereas enucleolated zygotes were capable of producing live pups and reconstructing normal nucleoli (Ogushi *et al.* 2008; Ogushi and Saitou 2010; Kyogoku *et al.* 2014*a*, 2014*b*). These findings support the idea that biochemical compositions of NPBs and NLBs differ: NLBs are comprised of molecular constituents that are necessary for early embryonic development, whereas NPBs do not contain them. In the present work, we showed that such constituents may include RNAs: indeed, RNA is easily detectable in oocyte NLBs (Fig. 3*a*), but is almost absent from zygotic NPBs (Figs 1*a*, *d*). RNAs lacking from zygotic NPBs may include maternally derived rRNA that is the major class of nucleolar RNA (Boisvert *et al.* 2007; Farley *et al.* 2015), mRNAs or regulatory non-coding RNAs that function at the zygotic stage (Zhang *et al.* 2014).

It is known that 35–40% of total RNA present in a fully grown mouse oocyte (0.4–0.6 ng per oocyte) degrades in MII oocytes or shortly after fertilisation and that the degraded RNAs include rRNA (Bachvarova *et al.* 1985; Paynton *et al.* 1988; Schultz 2002; Ihara *et al.* 2011). Nevertheless, a low amount of 28S rRNA becomes included in zygotic NPBs (Fig. 5*b*). This observation can explain the presence of a long-lived maternal RNA described in zygotic NPBs by autoradiography (Kopečný *et al.* 1995). The absence of nascent pre-rRNA and unprocessed rRNAs in zygotic NPBs is in line with literature on silencing of rDNA in one-cell embryos. From the other side, the lack of these rRNAs in zygotic NPBs implies that reforming nucleoli are mainly built of rRNAs transcribed from re-activated embryonic ribosomal genes. Like rRNAs, oocyte-derived nucleolar proteins also partially degrade after fertilisation (Fulka and Langerova 2014). However, the early rRNA processing factor and the main nucleolar methyltransferase fibrillarin (Fig. 7*a*, *j*), the rRNA processing factors NPM1 and nucleolin are included in zygotic NPBs (Fig. 5*a*; Fig. 7*c*, *e*, *k*). It is well known that in the mouse, the bulk re-activation of embryonic genes that are associated with ribosome biogenesis, occurs in late morula–blastocyst stages (Wang *et al.* 2004; Zeng and Schultz 2005; Hamatani *et al.* 2006). It is very likely therefore that maternal nucleolar proteins are utilised by maturing NPBs at least in two- and four-cell embryos. Indeed, on immunoblots of mouse embryos, the content of fibrillarin, NPM1 and nucleolin remains almost unchanged between the one-cell and four-cell stages (Fulka and Langerova 2014).

Taking into account literature data and the present results, we propose a scheme that illustrates assembly and maturation of

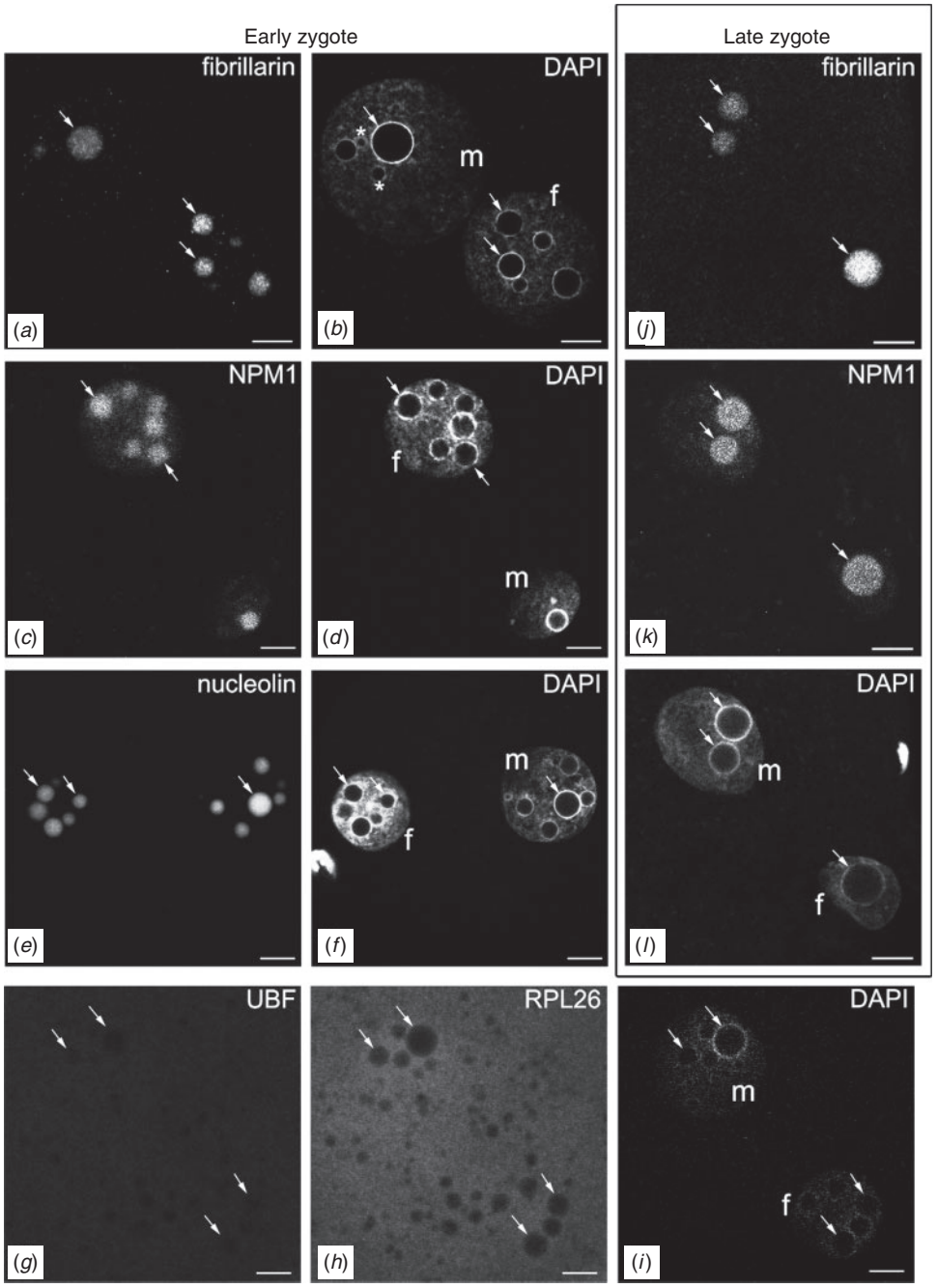

Fig. 7. Immunolabelling of NPBs (arrows) with antibodies against nucleolar proteins (*a*, *j*) fibrillarin, (*c*, *k*) NPM1, (*e*) nucleolin, (*g*) UBF and (*h*) the ribosomal protein RPL26 in (*a–i*) early and (*j–l*) late zygotes. Embryos were fixed with PFA, treated with proteinase K and processed for immunostaining as described in Materials and Methods. Before mounting in Vectashield, the embryos were counterstained with DAPI (*b*, *d*, *f*, *i*, *l*). The embryos shown in (*g–l*) were double immunolabelled for UBF and RPL26 (*g–i*) or for fibrillarin and NPM1 (*j–l*). f, female pronucleus; m, male pronucleus. Some early NPBs do not contain fibrillarin (*a*, *b*), asterisks. In all zygotic NPBs, UBF (*g*) and RPL26 (*h*) were not detected. Scale bars = 10 μm.

NPBs to functional nucleoli in early mouse embryos (Fig. 8). It implies that NPBs assembling in early zygotes are different in molecular composition. This assumption is based on the observations showing that some early zygotic NPBs are not associated with rRNA genes (Romanova *et al.* 2006*b*) and lack 28S rRNA (Fig. 5*b*) and the nucleolar protein fibrillarin (Fig. 7*a*). During the zygotic stage, NPBs fuse and become uniform in molecular composition yet remain impoverished for rRNAs. We assume

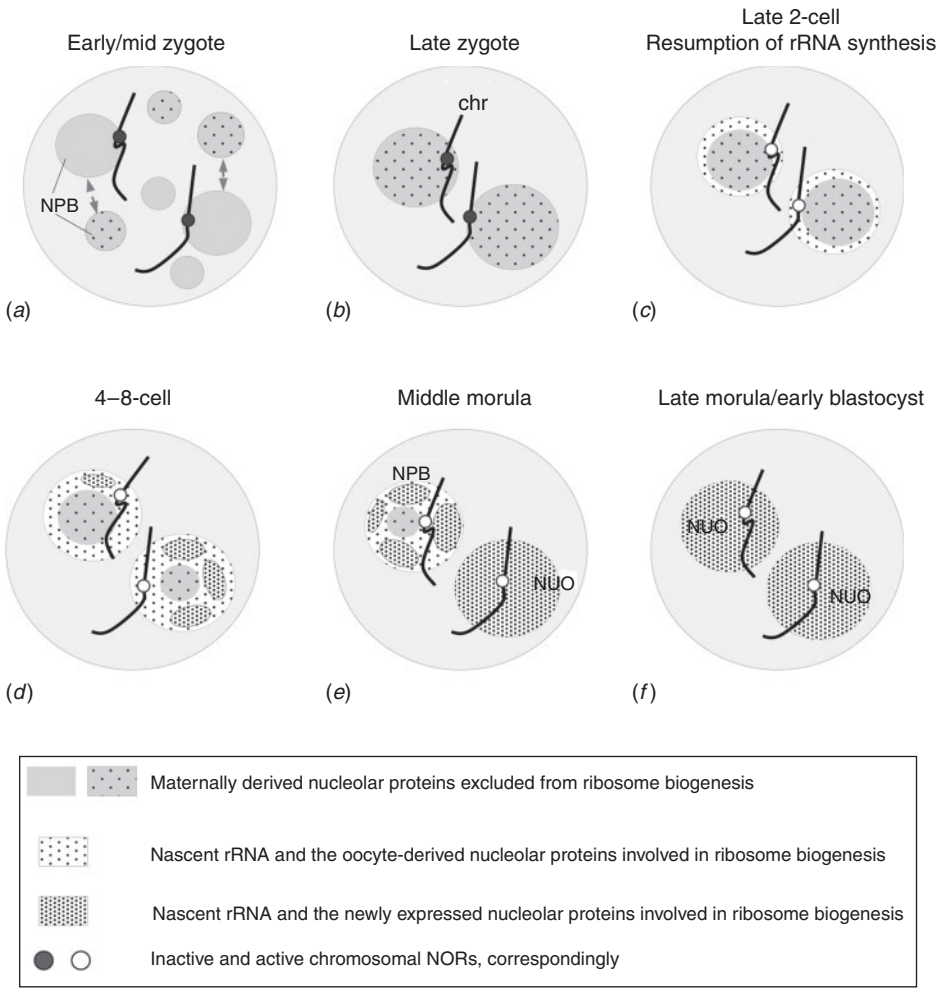

Fig. 8. A scheme illustrating the assembly of NPBs and their maturation to functional nucleoli at the subsequent stages of early embryonic development in the mouse. One pronucleus and two chromosomes are shown for simplicity. NPB, nucleolar precursor body; chr, chromosome; NUO, the normal nucleolus. (*a*) Early zygotic NPBs differ in molecular composition and may not be associated with chromosomal NORs. (*b*) During the zygotic stage, NPBs fuse (presumably around or close to the NORs) and become uniform in composition. (*c*) In late two-cell stage, activation of embryonic rRNA genes results in the appearance of nascent rRNAs on the NPB surface; the oocyte-derived nucleolar proteins are mainly involved in ribosome biogenesis. (*d*) In four–eight-cell embryos, NPBs utilise the newly synthesised rRNAs and the maternally inherited nucleolar proteins to make ribosomes that leads to (*d*, *e*) a gradual diminution of the NPB core. (*e*, *f*) When the global activation of the genes associated with ribosome biogenesis occurs, nucleoli consist of rRNAs and proteins expressed by an embryo.

that NPBs have a tendency to associate with chromosomal nucleolus-organising regions (NORs) and to nucleate assembly of nucleoli similar to the events in post-mitosis (Hernandez-Verdun 2011). Resumption of rRNA synthesis leads to the appearance of nascent rRNAs on the NPB surface and to translocation of the maternally derived nucleolar proteins to the sites of ribosome biogenesis (Fig. 8*c*). As a result, the NPB core containing maternal nucleolar proteins becomes gradually reduced (Fig. 8*d*, *e*). Starting from late morula–early blastocyst stages, functional tripartite nucleoli are comprised of rRNA and proteins, which are expression products of only embryonic genes (Fig. 8*f*).

Acknowledgements

This study was supported by the Russian Scientific Foundation (Grant number 14–14–00856). The authors are sincerely grateful to Dr Vladimir Mikoyan (the Moscow CRDF (USA) Global Office) for a critical reading of the manuscript.

References

Bachvarova, R., De Leon, V., Johnson, A., Kaplan, G., and Paynton, B. V. (1985). Changes in total RNA, polyadenylated RNA and actin mRNA during meiotic maturation of mouse oocytes. *Dev. Biol.* **108**, 325–331. doi:10.1016/0012-1606(85)90036-3

Baran, V., Veselá, J., Rehák, P., Koppel, J., and Fléchon, J. E. (1995). Localisation of fibrillarin and nucleolin in nucleoli of mouse

preimplantation embryos. *Mol. Reprod. Dev.* **40**, 305–310. doi:10.1002/MRD.1080400306

Biggiogera, M., Martin, T. E., Gordon, J., Amalric, F., and Fakan, S. (1994). Physiologically inactive nucleoli contain nucleoplasmic ribonucleoproteins: immunoelectron microscopy of mouse spermatids and early embryos. *Exp. Cell Res.* **213**, 55–63. doi:10.1006/EXCR.1994.1172

Bjerregaard, B., Wrenzycki, C., Strejcek, F., Laurincik, J., Holm, P., Ochs, R. L., Rosenkranz, C., Callesen, H., Rath, D., Niemann, H., and Maddox-Hyttel, P. (2004). Expression of nucleolar-related proteins in porcine preimplantation embryos produced *in vivo* and *in vitro*. *Biol. Reprod.* **70**, 867–876. doi:10.1095/BIOLREPROD.103.021683

Bogolyubova, I. O. (2011). Transcriptional activity of nuclei in two-cell blocked mouse embryos. *Tissue Cell* **43**, 262–265. doi:10.1016/J.TICE.2011.03.005

Boisvert, F.-M., Van Koningsbruggen, S., Navascués, J., and Lamond, A. I. (2007). The multifunctional nucleolus. *Nat. Rev. Mol. Cell Biol.* **8**, 574–585.

Bonnet-Garnier, A., Feuerstein, P., Chebrout, M., Fleurot, R., Jan, H. U., Debey, P., and Beaujean, N. (2012). Genome organisation and epigenetic marks in mouse germinal vesicle oocytes. *Int. J. Dev. Biol.* **56**, 877–887. doi:10.1387/IJDB.120149AB

Bouniol, C., Nguyen, E., and Debey, P. (1995). Endogenous transcription occurs at the one-cell stage in the mouse embryo. *Exp. Cell Res.* **218**, 57–62. doi:10.1006/EXCR.1995.1130

Braude, P., Bolton, V., and Moore, S. (1988). Human gene expression first occurs between the four- and eight-cell stages of preimplantation development. *Nature* **332**, 459–461. doi:10.1038/332459A0

Darzynkiewicz, Z., Kapuscinski, J., Traganos, F., and Crissman, H. A. (1987). Application of pyronin Y(G) in cytochemistry of nucleic acids. *Cytometry* **8**, 138–145. doi:10.1002/CYTO.990080206

Duncan, F. E., and Schultz, R. M. (2010). Gene expression profiling of mouse oocytes and preimplantation embryos. *Methods Enzymol.* **477**, 457–480. doi:10.1016/S0076-6879(10)77023-3

Engel, W., Zenzes, M. T., and Schmid, M. (1977). Activation of mouse ribosomal RNA genes at the two-cell stage. *Hum. Genet.* **38**, 57–63. doi:10.1007/BF00295808

Fakan, S., and Odartchenko, N. (1980). Ultrastructural organisation of the cell nucleus in early mouse embryos. *Biol. Cell.* **37**, 211–218.

Farley, K. I., Surovtseva, Y., Merkel, J., and Baserga, S. J. (2015). Determinants of mammalian nucleolar architecture. *Chromosoma*. doi:10.1007/S00412-015-0507-Z

Ferreira, J., and Carmo-Fonseca, M. (1995). The biogenesis of the coiled body during early mouse development. *Development* **121**, 601–612.

Fléchon, J. E., and Kopecný, V. (1998). The nature of the "nucleolus precursor body" in early preimplantation embryos: a review of fine-structure cytochemical, immunocytochemical and autoradiographic data related to nucleolar function. *Zygote* **6**, 183–191. doi:10.1017/S0967199498000112

Fulka, H., and Fulka, J., Jr (2010). Nucleolar transplantation in oocytes and zygotes: challenges for further research. *Mol. Hum. Reprod.* **16**, 63–67. doi:10.1093/MOLEHR/GAP088

Fulka, H., and Langerova, A. (2014). The maternal nucleolus plays a key role in centromere satellite maintenance during the oocyte-to-embryo transition. *Development* **141**, 1694–1704. doi:10.1242/DEV.105940

Geuskens, M., and Alexandre, H. (1984). Ultrastructural and autoradiographic studies of nucleolar development and rDNA transcription in preimplantation mouse embryos. *Cell Differ.* **14**, 125–134. doi:10.1016/0045-6039(84)90037-X

Graf, A., Krebs, S., Heininen-Brown, M., Zakhartchenko, V., Blum, H., and Wolf, E. (2014). Genome activation in bovine embryos: review of the literature and new insights from RNA sequencing experiments. *Anim. Reprod. Sci.* **149**, 46–58. doi:10.1016/J.ANIREPROSCI.2014.05.016

Hamatani, T., Ko, M. Sh., Yamada, M., Kuji, N., Mizusawa, Y., Shoji, M., Hada, T., Asada, H., Maruyama, T., and Yoshimura, Y. (2006). Global gene expression profiling of preimplantation embryos. *Hum. Cell* **19**, 98–117. doi:10.1111/J.1749-0774.2006.00018.X

Hernandez-Verdun, D. (2011). Assembly and disassembly of the nucleolus during the cell cycle. *Nucleus* **2**, 189–194. doi:10.4161/NUCL.2.3.16246

Hyttel, P., Laurincik, J., Viuff, D., Fair, T., Zakhartchenko, V., Rosenkranz, C., Avery, B., Rath, D., Niemann, H., Thomsen, P. D., Schellander, K., Callesen, H., Wolf, E., Ochs, R. L., and Greve, T. (2000). Activation of ribosomal RNA genes in preimplantation cattle and swine embryos. *Anim. Reprod. Sci.* **60–61**, 49–60. doi:10.1016/S0378-4320(00)00087-7

Ihara, M., Tseng, H., and Schultz, R. M. (2011). Expression of variant ribosomal RNA genes in mouse oocytes and preimplantation embryos. *Biol. Reprod.* **84**, 944–946. doi:10.1095/BIOLREPROD.110.089680

Kapuscinski, J., and Darzynkiewicz, Z. (1987). Interactions of pyronin Y(G) with nucleic acids. *Cytometry* **8**, 129–137. doi:10.1002/CYTO.990080205

Kopečný, V., Landa, V., and Pavlok, A. (1995). Localisation of nucleic acids in the nucleoli of oocytes and early embryos of mouse and hamster: an autoradiographic study. *Mol. Reprod. Dev.* **41**, 449–458. doi:10.1002/MRD.1080410407

Kyogoku, H., Kitajima, T. S., and Miyano, T. (2014*a*). Nucleolus precursor body (NPB): a distinct structure in mammalian oocytes and zygotes. *Nucleus* **5**, 493–498. doi:10.4161/19491034.2014.990858

Kyogoku, H., Fulka, J., Wakayama, T., and Miyano, T. (2014*b*). *De novo* formation of nucleoli in developing mouse embryos originating from enucleolated zygotes. *Development* **141**, 2255–2259. doi:10.1242/DEV.106948

Laurincik, J., Thomsen, P. D., Hay-Schmidt, A., Avery, B., Greve, T., Ochs, R. L., and Hyttel, P. (2000). Nucleolar proteins and nuclear ultrastructure in preimplantation bovine embryos produced *in vitro*. *Biol. Reprod.* **62**, 1024–1032. doi:10.1095/BIOLREPROD62.4.1024

Laurincik, J., Schmoll, F., Mahabir, E., Schneider, H., Stojkovic, M., Zakhartchenko, V., Prelle, K., Hendrixen, P. J., Voss, P. L., Moeszlacher, G. G., Avery, B., Dieleman, S. J., Besenfelder, U., Müller, M., Ochs, R. L., Wolf, E., Schellander, K., and Maddox-Hyttel, P. (2003). Nucleolar proteins and ultrastructure in bovine *in vivo*-developed, *in vitro*-produced and parthenogenetic cleavage-stage embryos. *Mol. Reprod. Dev.* **65**, 73–85. doi:10.1002/MRD.10294

Lazdins, I. B., Delannoy, M., and Sollner-Webb, B. (1997). Analysis of nucleolar transcription and processing domains and pre-rRNA movements by *in situ* hybridisation. *Chromosoma* **105**, 481–495. doi:10.1007/BF02510485

Li, J.-J., Lian, H.-Y., Zhang, S.-Y., Cui, W., Sui, H.-S., Han, D., and Liu, N. (2012). Regulation of fusion of the nucleolar precursor bodies following activation of mouse oocytes: roles of the maturation-promoting factors and mitogen-activated protein kinases. *Zygote* **20**, 291–303. doi:10.1017/S0967199411000219

Morris, S. A., and Zernicka-Goetz, M. (2012). Formation of distinct cell types in the mouse blastocyst. *Results Probl. Cell Differ.* **55**, 203–217. doi:10.1007/978-3-642-30406-4_11

Mullineux, S. T., and Lafontaine, D. L. (2012). Mapping the cleavage sites on mammalian pre-rRNAs: where do we stand? *Biochimie* **94**, 1521–1532. doi:10.1016/J.BIOCHI.2012.02.001

Oestrup, O., Hall, V., Petkov, S. G., Wolf, X. A., Hyldig, S., and Hyttel, P. (2009). From zygote to implantation: morphological and molecular dynamics during embryo development in the pig. *Reprod. Domest. Anim.* **44**(Suppl. 3), 39–49. doi:10.1111/J.1439-0531.2009.01482.X

Ogushi, S., and Saitou, M. (2010). The nucleolus in the mouse oocyte is required for the early step of both female and male pronucleus organisation. *J. Reprod. Dev.* **56**, 495–501. doi:10.1262/JRD.09-184H

Ogushi, S., Palmieri, C., Fulka, H., Saitou, M., Miyano, T., and Fulka, J., Jr (2008). The maternal nucleolus is essential for early embryonic development in mammals. *Science* **319**, 613–616. doi:10.1126/SCIENCE.1151276

Papale, L., Fiorentino, A., Montag, M., and Tomasi, G. (2012). The zygote. *Hum. Reprod.* **27**, i22–i49. doi:10.1093/HUMREP/DES205

Paynton, B. V., Rempel, R., and Bachvarova, R. (1988). Changes in state of adenylation and time course of degradation of maternal mRNAs during oocyte maturation and early embryonic development in the mouse. *Dev. Biol.* **129**, 304–314. doi:10.1016/0012-1606(88)90377-6

Rodriguez-Zas, S. L., Schellander, K., and Lewin, H. A. (2008). Biological interpretations of transcriptomic profiles in mammalian oocytes and embryos. *Reproduction* **135**, 129–139. doi:10.1530/REP-07-0426

Romanova, L. G., Anger, M., Zatsepina, O. V., and Schultz, R. M. (2006*a*). Implication of nucleolar protein SURF6 in ribosome biogenesis and preimplantation mouse development. *Biol. Reprod.* **75**, 690–696. doi:10.1095/BIOLREPROD.106.054072

Romanova, L., Korobova, F., Noniashvilli, E., Dyban, A., and Zatsepina, O. (2006*b*). High-resolution mapping of ribosomal DNA in early mouse embryos by fluorescence *in situ* hybridisation. *Biol. Reprod.* **74**, 807–815. doi:10.1095/BIOLREPROD.105.047340

Schultz, R. M. (2002). The molecular foundations of the maternal to zygotic transition in the preimplantation embryo. *Hum. Reprod.* **8**, 323–331. doi:10.1093/HUMUPD/8.4.323

Shishova, K. V., Lavrentyeva, E. A., Dobrucki, J. W., and Zatsepina, O. V. (2015). Nucleolus-like bodies of fully grown mouse oocytes contain key nucleolar proteins but are impoverished for rRNA. *Dev. Biol.* **397**, 267–281. doi:10.1016/J.YDBIO.2014.11.022

Svarcova, O., Dinnyes, A., Polgar, Z., Bodo, S., Adorjan, M., Meng, Q., and Maddox-Hyttel, P. (2009). Nucleolar re-activation is delayed in mouse embryos cloned from two different cell lines. *Mol. Reprod. Dev.* **76**, 132–141. doi:10.1002/MRD.20936

Tesarík, J., Kopecný, V., Plachot, M., and Mandelbaum, J. (1987). High-resolution autoradiographic localisation of DNA-containing sites and RNA synthesis in developing nucleoli of human preimplantation embryos: a new concept of embryonic nucleogenesis. *Development* **101**, 777–791.

Vogt, E. J., Meglicki, M., Hartung, K. I., Borsuk, E., and Behr, R. (2012). Importance of the pluripotency factor LIN28 in the mammalian nucleolus during early embryonic development. *Development* **139**, 4514–4523. doi:10.1242/DEV.083279

Wang, Q. T., Piotrowska, K., Ciemerych, M. A., Milenkovic, L., Scott, M. P., Davis, R. W., and Zernicka-Goetz, M. (2004). A genome-wide study of gene activity reveals developmental signalling pathways in the preimplantation mouse embryo. *Dev. Cell* **6**, 133–144. doi:10.1016/S1534-5807(03)00404-0

Zatsepina, O. V., Voit, R., Grummt, I., Spring, H., Semenov, M. V., and Trendelenburg, M. F. (1993). The RNA polymerase I-specific transcription initiation factor UBF is associated with transcriptionally active and inactive ribosomal genes. *Chromosoma* **102**, 599–611. doi:10.1007/BF00352307

Zatsepina, O. V., Bouniol-Baly, C., Amirand, C., and Debey, P. (2000). Functional and molecular reorganisation of the nucleolar apparatus in maturing mouse oocytes. *Dev. Biol.* **223**, 354–370. doi:10.1006/DBIO.2000.9762

Zatsepina, O., Baly, C., Chebrout, M., and Debey, P. (2003). The step-wise assembly of a functional nucleolus in preimplantation mouse embryos involves the Cajal (coiled) body. *Dev. Biol.* **253**, 66–83. doi:10.1006/DBIO.2002.0865

Zeng, F., and Schultz, R. M. (2005). RNA transcript profiling during zygotic gene activation in the preimplantation mouse embryo. *Dev. Biol.* **283**, 40–57. doi:10.1016/J.YDBIO.2005.03.038

Zhang, K., Huang, K., Luo, Y., and Li, S. (2014). Identification and functional analysis of long non-coding RNAs in mouse cleavage stage embryonic development based on single-cell transcriptome data. *BMC Genomics* **15**, 845. doi:10.1186/1471-2164-15-845